Accepted Manuscript

A novel series of napabucasin derivatives as orally active inhibitors of signal transducer and activator of transcription 3 (STAT3)

Chungen Li, Caili Chen, Qi An, Tao Yang, Zitai Sang, Yang Yang, Yuan Ju, Aiping Tong, Youfu Luo

PII: S0223-5234(18)30944-9

DOI: https://doi.org/10.1016/j.ejmech.2018.10.067

Reference: EJMECH 10853

To appear in: *European Journal of Medicinal Chemistry*

Received Date: 30 July 2018

Revised Date: 29 October 2018

Accepted Date: 30 October 2018

Please cite this article as: C. Li, C. Chen, Q. An, T. Yang, Z. Sang, Y. Yang, Y. Ju, A. Tong, Y. Luo, A novel series of napabucasin derivatives as orally active inhibitors of signal transducer and activator of transcription 3 (STAT3), *European Journal of Medicinal Chemistry* (2018), doi: https://doi.org/10.1016/j.ejmech.2018.10.067.

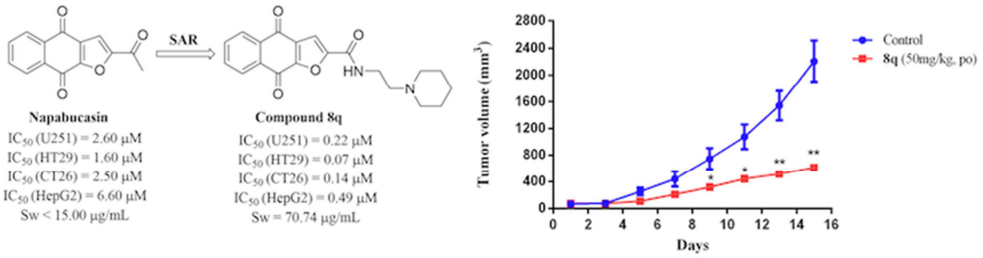

A Novel Series of Napabucasin Derivatives as Orally Active Inhibitors of Signal Transducer and Activator of Transcription 3 (STAT3)

Chungen Li[1], Caili Chen[1], Qi An[1], Tao Yang, Zitai Sang, Yang Yang, Yuan Ju, Aiping Tong[*], Youfu Luo[*]

State Key Laboratory of Biotherapy and Cancer Center, West China Hospital, West China Medical School, Sichuan University, and Collaborative Innovation Center for Biotherapy, Chengdu, 610041, China

[1] These authors contributed equally to this work.

* Corresponding authors.

E-mail addresses: luo_youfu@scu.edu.cn, aipingtong@scu.edu.cn

Highlights

1. *In vitro*, compound **8q** was over 10-fold more potent than **napabucasin** on U251, HepG2, HT29 and CT26 cells.
2. In mouse model of colorectal cancer, **8q** significantly reduced tumor growth. The TGI of **8q** at 50 mg/kg was 63 %.
3. Compound **8q** has a K_D of 110.2 nM for full-length STAT3 recombinant protein by surface plasmon resonance analysis.
4. The aqueous solubility of **8q** was over 4.5-fold higher than that of **napabucasin**.
5. Compound **8q** exhibited good safety profile in BALB/c mice model.

Abstract

The transcription factor STAT3 is an attractive target for a variety of cancers therapy. Napabucasin, applied in phase III clinical trials for the treatment of a variety of cancers, was regarded as one of the most promising anticancer drug by targeting STAT3. Herein, a novel series of napabucasin derivatives were designed and synthesized, which presented a potent inhibitory activity on a variety of cancers cells. Among the derivatives compound **8q** exhibited potent inhibitory activity on U251, HepG2, HT29 and CT26 cells with the IC_{50} values of 0.22, 0.49, 0.07 and 0.14 μM, respectively, which was over 10-fold more potent than napabucasin. Treatment with compound **8q** decreased protein expression level of total STAT3 and p-STAT3^{Y705} *in vitro*. The binding of compound **8q** with STAT3 were further validated by

electrophoretic mobility shift assay and surface plasmon resonance analysis. Compound **8q** has a K_D of 110.2 nM for full-length STAT3 recombinant protein. Moreover, the aqueous solubility of **8q** was over 4.5-fold than that of napabucasin. In addition, compound **8q** *in vivo* significantly reduced tumor growth compared to untreated mice, and exhibited good safety profile, indicating its great potential as an efficacious drug candidate for oncotherapy.

Key words: antitumor activity, STAT3 inhibitors, napabucasin derivatives.

1. Introduction

Signal transducer and activator of transcription 3 (STAT3), a STAT protein family member [1], is an oncogene being frequently activated in numerous cancers, such as glioma, lung, liver and other cancers [2]. It plays a critical role in some cellular processes such as cell growth and apoptosis by mediating the expression of target genes [3]. Furthermore, evidences from recent studies have indicated that STAT3 was related with the regulation of tumor microenvironment and tumor stem cell, suggesting an important role for STAT3 inhibitors in the self-renewal and differentiation of tumor stem cell and immunotherapy [4]. Thus, inhibiting the activation of STAT3 is an effective strategy in the cancer therapies, and the STAT3 may be used widely as one of the most promising anticancer target.

Over the past few years, there were significant advances in the discovery of STAT3 inhibitors [5, 6]. Several potent compounds have been discovered and promoted to early phase of drug development pipelines, such as **niclosamide**, **HJC0152**, **stattic**, **STX-0119**, **STA-21**, **LLL12**, **LY-5**, **napabucasin** [7-14] (**Figure 1**).

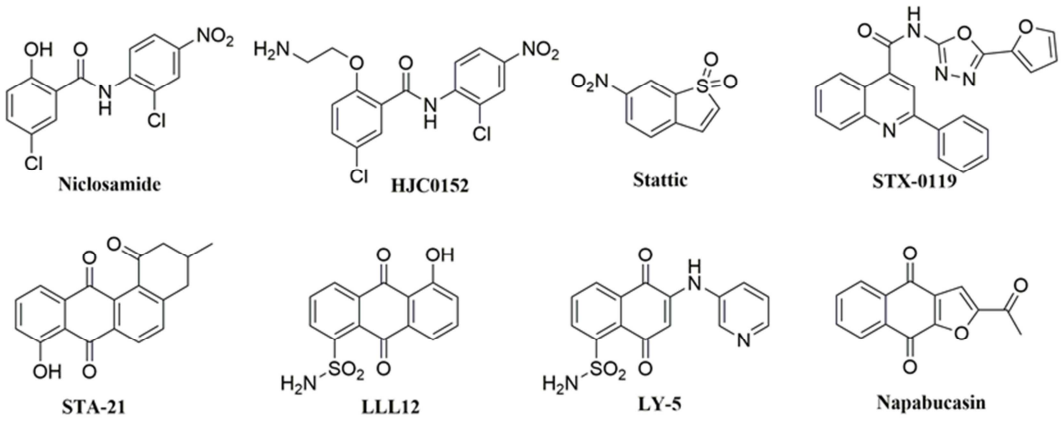

Figure 1. Representative small-molecule STAT3 inhibitors

Napabucasin, an excellent STAT3 small molecule inhibitor by targeting and blocking cancer stem cell pathway activity, which was applied in phase III clinical trials for the treatment of a variety of cancers such as metastatic colorectal carcinoma, pancreatic cancer, gastric cancer and non-small cell lung cancer [15-17]. Napabucasin was regarded as one promising lead compound to generate novel STAT3 inhibitors [18]. Several new anticancer derivatives of napabucasin were developed through chemical structural modifications toward napabucasin in recent years [19-21] (**Figure 2)**.

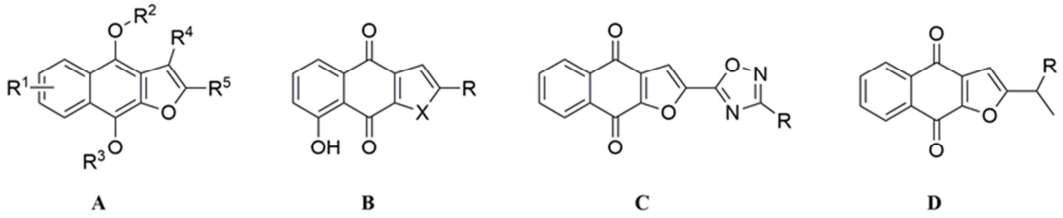

Figure 2. Representative napabucasin derivatives

To seek napabucasin derivatives with enhanced physicochemical properties, it is necessary to identify the position suitable to modify in the scaffold. Napabucasin was docked into STAT3 protein (PDB code: 1BG1). The acetyl group at 2-position of furan ring protrudes towards the receptor surface, indicating that it is a good site to conduct structural modification and the binding affinity will not decreases. In our first series of compounds, α, β-Unsaturated ketone was selected as a linker for its extensive application in antitumor drugs, for example curcumin (**Figure 3)**. The second series of napabucasin derivatives was introduced with hydrophilic groups, such as piperidyl,

pyrazinyl, and substituted amino groups by an amidation reaction.

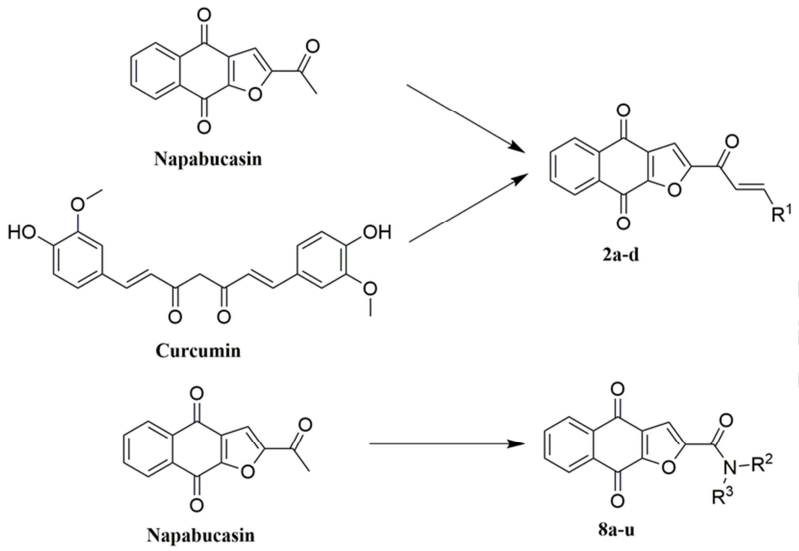

Figure 3. The design concept of the target compounds

2. Results and discussion

2.1. Chemistry

The synthesis of **2a-d** was carried out following the procedures shown in **Scheme 1**. The compounds **2a-d** were prepared by aldol condensation reaction between commercially available 2-acetylnaphtho[2,3-b]furan-4,9-dione (**1**) and substituted aromatic aldehydes under the condition of piperidine in ethanol. As illustrated in **Scheme 2**, compounds **8a-u** were prepared starting from reaction of 2-hydroxy-1,4-naphthoquinone (**3**) with iodobenzene diacetate to give intermediate 3-phenyliodonio-1,2,4-trioxo-1,2,3,4-tetrahydronaphthalenide (**4**). Then cyclization reaction between **4** with propargyl alcohol afforded 2-hydroxymethyl-naphtho[2,3-*b*]furan-4,9-dione (**5**). The subsequent oxidation reaction of **5** with pyridinium chlorochromate (PCC) yielded 2-formyl-4,9-dihydronaphtho[2,3-*b*]-furan-4,9-dione (**6**), which was further oxidized to the 4,9-dioxo-4,9-dihydronaphtho[2,3-b]furan-2-carboxylic acid **(7)** by H_2O_2 and glacial acetic acid. Finally, amidation reaction of intermediate compound **7** with different substituted alkyl amines or *N*-heterocycles to give target compounds **8a-u**.

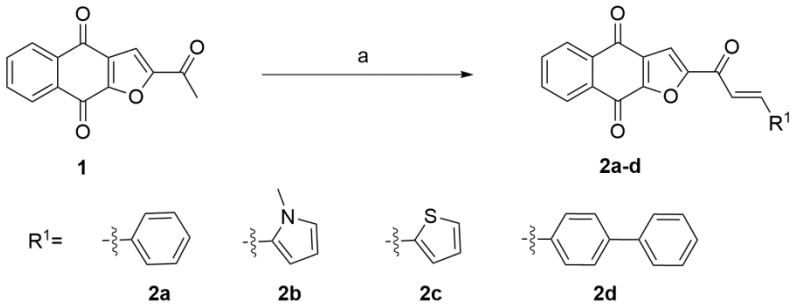

Scheme 1. Synthesis of **2a-d**. Reagents and conditions: (a) piperidine, EtOH, reflux, 6-12h.

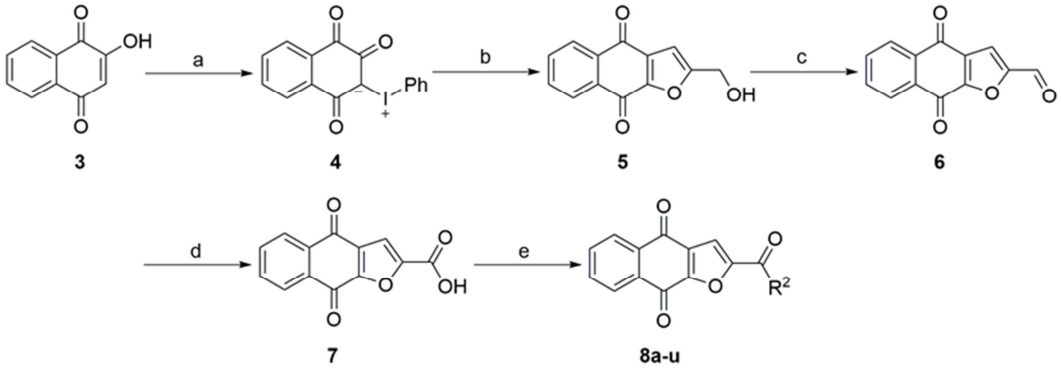

Scheme 2. Synthesis of **8a-u**. Reagents and conditions: (a) $PhI(OAc)_2$, $CHCl_3$, 5 h. (b) Propargyl alcohol, Cu_2O, 80°C, 2 h. (c) PCC, CH_2Cl_2, r.t., overnight. (d) H_2O_2 30%, AcOH, 75 °C, 4h. (e) HATU, Et_3N, r.t., 2h.

2.2. *In vitro* cell growth inhibitory activity

To evaluate the anticancer activities of the synthetic compounds, three STAT3 over- activated human cancer cell lines (U251, HepG2 and HT29 cells) and mice CT-26 cells were examined (**Table 1**). The inhibitory activity of compounds **2a** and **2d** were significantly decreased compared with that of napabucasin. **2b** and **2c**, which were substituted with heterocyclic groups, maintained the inhibitory activities in U251 and HT29 cells with the IC_{50} values of 0.87-2.20 μM. But the activities of **2b** and **2c** had not been improved compared with that of napabucasin, indicating that aromatic substitution was adverse to improve activity, and substitution of heterocyclic groups was favorable for the inhibitory activity.

Replaced with heterocyclic alkyl group at R^2 position (**8a-g)** was tolerated. The inhibitory activity of compound **8f**, substituted with the 4-ethylpiperazin-1-yl at R^2 position, was increased for U251, HT29 and CT26 cells with the IC_{50} values of 0.87, 0.21, and 0.59 μM, respectively. However, the compounds **8h-l**, substituted with big size on the cyclic amine, exhibited declined inhibitory activity. It demonstrated that the substitutions with small size on the cyclic amine were beneficial to improve

inhibitory activity.

Compound **8q,** with 2-(piperidin-1-yl)ethylamino- group substituted at the R^2 position, inhibited the growth of U251, HepG2, HT29 and CT26 cells with the IC_{50} values of 0.22, 0.49, 0.07 and 0.14 μM, respectively. The values were lowered over 10-fold compare with napabucasin. When the corresponding position transformed to aromatic alkyl amine (**8s-u**), the inhibitory activity declined obviously, suggesting that the aromatic alkyl substitution at R^2 position was not versatile to improve activity. Moreover, to evaluate the selectivity, the effects of the derivatives on STAT3-negative prostate cancer PC-3 cell line were examined. As a result, the IC_{50} values of 16 derivatives were over 10 μM and the remaining 10 derivatives and napabucasin were over 2 μM.

Table 1 Activity of compounds *in vitro*

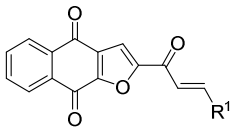

2a-d

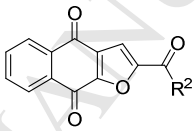

8a-u

Cpd.	R^1/ R^2	IC_{50} ±SD [a] (μM)				
		U251	HepG2	HT29	CT26	PC-3
2a		>10	>10	>10	>10	>10
2b		1.50±0.25	>10	0.87±0.01	2.48±0.07	>10
2c		2.20±0.06	>10	1.52±0.01	>10	>10
2d	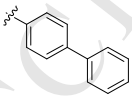	>10	>10	>10	>10	>10
8a		2.18±0.11	>10	1.08±0.03	0.58±0.05	9.65±1.24
8b		2.16±0.11	>10	1.57±0.01	0.95±0.14	>10
8c		2.19±0.09	7.30±0.06	0.86±0.11	0.57±0.04	6.84±0.71
8d		3.10±0.04	9.63±0.15	1.65±0.13	1.35±0.24	5.83±0.74

8e	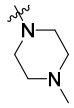	1.37±0.02	5.27±0.13	0.39±0.09	0.26±0.05	4.58±0.62
8f		0.87±0.03	>10	0.21±0.01	0.59±0.06	2.06±0.30
8g	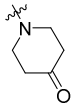	0.58±0.02	2.50±0.05	1.13±0.02	0.61±0.03	>10
8h	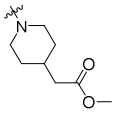	5.92±0.43	9.66±0.31	>10	-	>10
8i	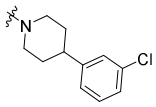	>10	>10	>10	-	>10
8j	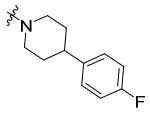	>10	>10	>10	-	>10
8k	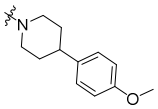	>10	>10	>10	-	9.64±1.13
8l	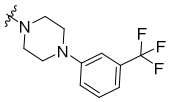	>10	>10	>10	-	>10
8m	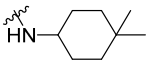	2.65±0.43	11.25±0.36	>10	-	>10
8n	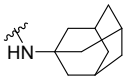	>10	>10	>10	-	>10
8o	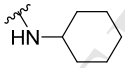	3.02±0.09	>10	>10	-	>10
8p	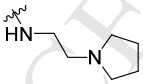	0.90±0.08	1.75±0.22	0.30±0.38	0.20±0.27	4.45±0.69
8q	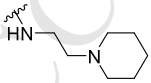	0.22±0.03	0.49±0.04	0.07±0.001	0.14±0.01	4.13±0.46
8r	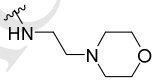	1.63±0.33	>10	0.37±0.01	0.05±0.009	7.19±0.82
8s	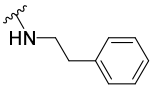	>10	>10	>10	-	>10
8t	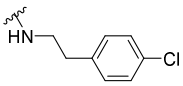	3.36±0.57	>10	>10	-	>10
8u	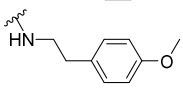	6.32±0.62	>10	>10	-	>10
Napabucasin	-	2.60±0.38	6.60±0.36	1.60±0.11	2.50±0.09	5.25±0.57

[a] Values were the average of at least three separate determinations (Mean ± SD). Dash (-) indicates not determined.

2.3. Molecular docking

To explore the possible interaction modes of compounds with STAT3, molecular docking studies were performed in Discovery Studio (DS) 3.1. As shown in **Figure 4**, napabucasin could bind to the STAT3 (PDB code: 1BG1) SH2 domain by hydrogen bonds with Arg609 and Arg595 residues. Furthermore, napabucasin was formed cation-π interactions with Ser636 and Lys591 residues. The representative compound **8q** not only formed hydrogen bonds with Arg609 and Arg595 residues, but also new hydrogen bonds with Lys591 and Arg595 residues, and it also formed cation-π interactions with the Ser636 and Lys591 residues. The result of the docking study indicated that compound **8q** matched perfectly with the configuration of the SH2 domain of STAT3, providing a rationale explaining the excellent activity of compound **8q**.

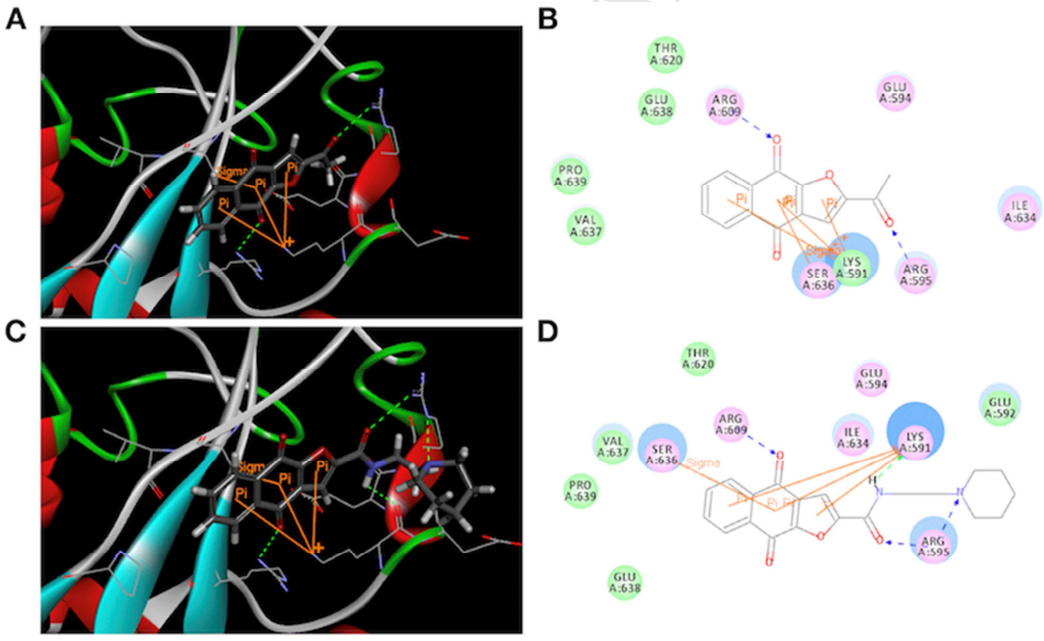

Figure 4. The binding mode of napabucasin, **8q** and STAT3 SH2 domain. **(A)** Napabucasin in 3D representation. **(B)** Napabucasin in 2D representation. **(C) 8q** in 3D representation **(D) 8q** in 2D representation. Hydrogen bond is shown in green and blue dash lines in 3D and 2D representation, respectively.

2.4. The physicochemical properties of several final compounds

The aqueous solubility was tested by HPLC method, and the Clog P was calculated by ChemBioDraw Ultra 14.0. The aqueous and lipid solubility of most compounds were improved (**Table 2**). For example, the solubility of compound **8q**

and **8e** was improved to 70.7 and 109.4 μg/mL, respectively. Compounds **8q** and **8e,** with introduction of basic amino groups to R^2 position, were beneficial to increase the water-solubility.

Table 2 Aqueous solubility of compounds **8c**-**g**, **8q** and **8r**

Cpd.	Structure	Clog P [a]	Aqueous solubility ±SD [b] (μg/mL)	Aqueous solubility ±SD (μM)
8c	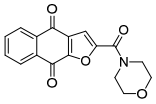	1.38	50.4±0.95	162.1±3.05
8d	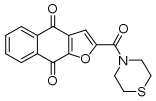	2.11	<25.0	<76.5
8e	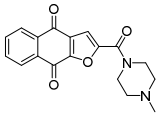	1.94	109.4±3.76	337.4±11.60
8f	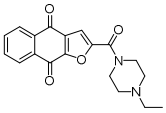	2.47	81.5±0.98	240.9±2.89
8g	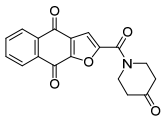	1.32	38.1±2.38	117.7±7.36
8q	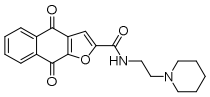	3.28	70.7±0.50	200.9±1.42
8r	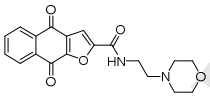	2.07	<25.0	<70.6
Napabucasin	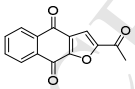	1.66	<15.0	<62.5

[a] Octanol-water partition coefficient (log P) was calculated by ChemBioDraw Ultra 14.0.

[b] Values were the average of at least three separate determinations (Mean ± SD).

2.5. *In Vivo* Antitumor Activity Evaluation

The amino acid sequence of STAT3 is conserved between human and mice. And the antitumor effects of STAT3 inhibitor is partly depend on its regulation of the immune systems [22]. Thus, to evaluate the effects of STAT3 inhibitors, immunocompetent mice are always used as animal model. Consistently, our data also show that STAT3 inhibitor exhibit efficacy both in human colorectal cancer cell line HT29 and in mouse colorectal cancer cell line CT26 (**Table 1**). To further investigate

the antitumor potential *in vivo*, we evaluated the effects of compound **8q** in CT26 mouse tumor model. As shown in **Figure 5**, compound **8q** exhibited potent oral antitumor activity compared with the control. The tumor growth delay induced by **8q** was visualized by the final tumor tissue size in **Figure 5A** and the tumor growth curve in **Figure 5B**. The TGI (tumor growth inhibition) and T/C (relative increment ratio) with **8q** at 50 mg/kg were 63% and 28%, respectively.

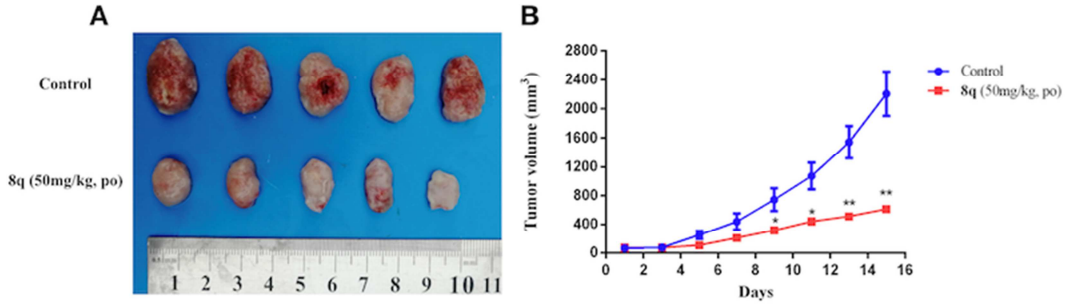

Figure 5. (A) Anatomical mice's tumor tissues treated with **8q** and vehicle**. (B)** Growth curves of mice's tumor volume (Mean ± SD, n = 5; *, $p < 0.05$, **, $p < 0.01$).

2.6. Preliminary safety profile of compound 8q

Compound **8q** was well tolerated and no significant difference of body weights was observed between control and **8q** treated mice (**Figure S1**). All mice survived without apparent behavioral alterations or other side effects.

Furthermore, the pathological change in major organs was examined by H&E staining. As shown in **Figure 6**, the histology of the heart, liver, spleen, lung and kidney indicated that the cells of organ tissues from the **8q** treated group kept a complete morphology, without obvious cellular inflammatory, edema or necrosis, implying no noticeable toxicity to the five major organs.

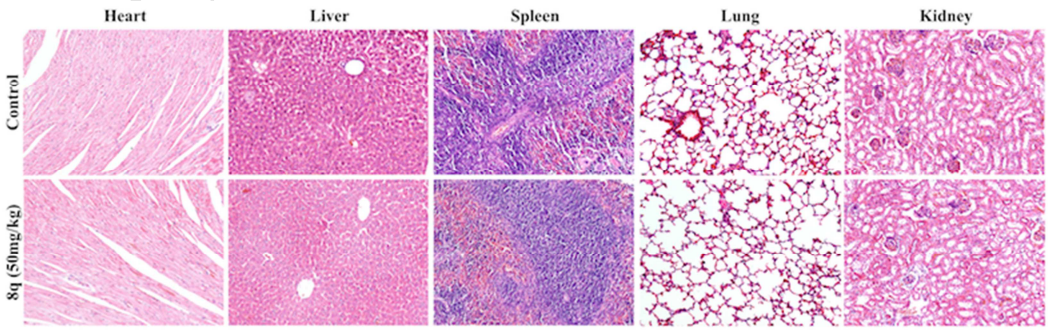

Figure 6. Histological section of anatomical heart, liver, spleen, lung and kidney stained with

H&E from colorectal cancer model mice treated with compound **8q**.

2.7. Compound 8q decrease protein expression of total STAT3 and p-STAT3^{Y705}

To gain insight into the mechanism of compound **8q**, we conducted western blot, immunofluorescence and sandwich enzyme-linked immunosorbent assays to examine the protein expression level of total and p-STAT3^{Y705} in U251 and HepG2 after treatment. As shown in **Figure 7A**, decrease of both total STAT3 and p-STAT3^{Y705} was observed at 200 nM concentrations after 24 hours of treatment in U251 and HepG2 cells. Through immunofluorescence staining, the expression of total STAT3 decreased obviously in HepG2 cells treated with **8q** (400 nM) for 24 h (**Figure 7B**). Furthermore, we evaluated the total and p-STAT3^{Y705} levels in U251 and HepG2 cells by sandwich enzyme-linked immunosorbent assay. As shown, both total STAT3 and p-STAT3^{Y705} decreased significantly after treatment with **8q** (200 nM for U251 and 400 nM for HepG2 cells) for 24 h or 48 h (**Figure 7C**, **D**).

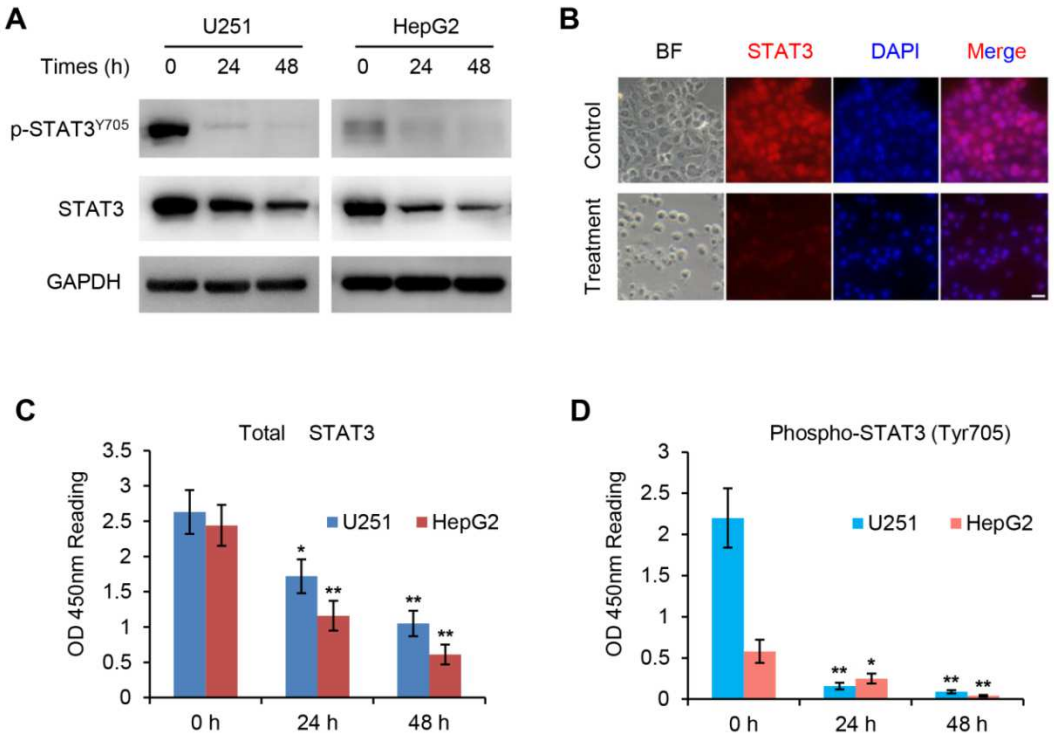

Figure 7. 8q treatment decrease protein expression level of total STAT3 and p-STAT3^{Y705} *in vitro*. **(A)** Western blot analysis of STAT3 and p-STAT3^{Y705} in U251 and HepG2 cells treated with **8q** (200 nM for U251 and 400 nM for HepG2 cells) for 24 and 48 h. **(B)** Immunofluorescence analysis of total STAT3 in HepG2 cells treated with **8q** (400 nM) for 24 h. Images were taken on a Zeiss inverted microscope with 20× objective lens. BF, Bright-Field. Scale bar: 50μm. **(C, D)**

Sandwich enzyme-linked immunosorbent assay of total and p-STAT3^{Y705} in U251 and HepG2 cells treated with **8q** (200 nM for U251 and 400 nM for HepG2 cells) for 24 and 48 h. Error bars represent standard deviations. Paired t-test was used for statistical analyses of treatment groups compared with control group. *, p< 0.05; **, p< 0.01.

2.8. Binding of Compound 8q with STAT3

Furthermore, we validate the binding of compound **8q** with STAT3 using EMSA and SPR analysis. As shown in **Figure 8A**, compound **8q** incubation at 100 nM and 200 nM concentration dramatically decreased the binding of STAT3 with biotin-labeled DNA probe. SPR analyses with Biacore X100 also show that compound **8q** has a K_D of 110.2 nM for full-length STAT3 recombinant protein (**Figure 8B**).

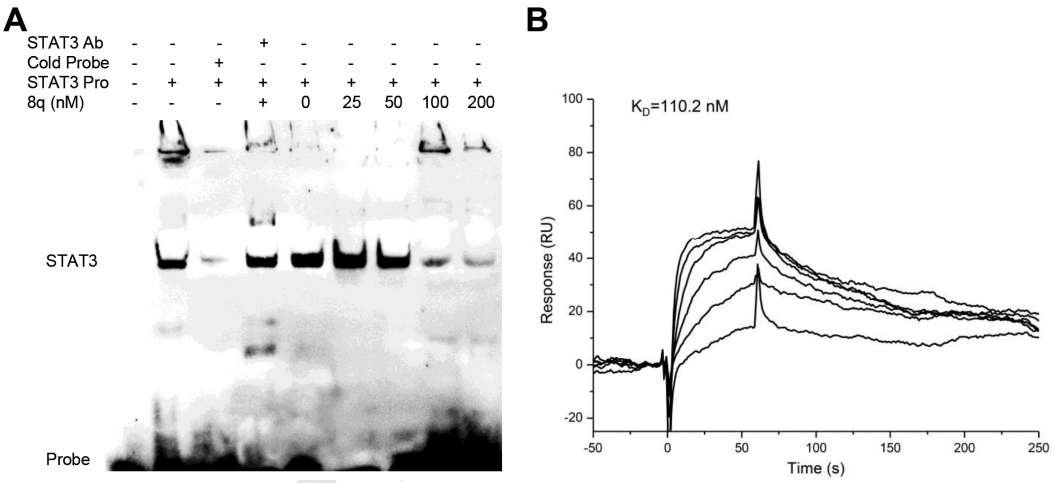

Figure 8. Electrophoretic mobility shift assay (EMSA) and surface plasmon resonance (SPR) analysis. **(A)** The effects of compound **8q** on the DNA binding activity of STAT3 was determined by EMSA with biotin-labeled DNA probe and Flag-tagged STAT3 pull-downed from HEK293T cells transiently transfected with full-length STAT3 cDNA. Ab, antibody; Pro, protein. **(B)** STAT3 and compound **8q** binding analyses with Biacore X100. The concentrations of **8q** are varied from 18.75 nM to 600 nM. The equilibrium dissociation constant (K_D) was obtained by using the GE BIA evaluation 2.0 software.

3. Conclusion

In summary, a novel series of napabucasin derivatives were designed, synthesized and biologically evaluated. Most of the designed compounds exerted promising inhibitory activity on U251, HepG2, HT29 and CT26 cells, and exhibited

improved solubility compared with napabucasin. The most potent compound **8q** exhibited remarkable inhibitory activity on U251, HepG2, HT29 and CT26 cells with the IC_{50} values of 0.22, 0.49, 0.07 and 0.14 μM, respectively. In mouse model of colorectal cancer, **8q** significantly inhibited tumor growth. Treatment with compound **8q** decreased protein expression level of total STAT3 and p-STAT3^{Y705} *in vitro*. The binding of compound **8q** with STAT3 were validated by EMSA and SPR analysis. Compound **8q** has a K_D of 110.2 nM for full-length STAT3 recombinant protein. Molecular docking suggested that compound **8q** bound to the SH2 domain of STAT3. Together, compound **8q** is worth of further investigations toward the discovery of STAT3 inhibitor as a drug candidate for oncotherapy.

4. Experimental section

4.1. Chemistry

All common reagents and solvents were obtained from commercial suppliers and used without further purification. Reaction progress was monitored using analytical thin layer chromatography (TLC) on precoated silica gel 60 F254 plates (0.25 mm, Qingdao Haiyang Inc.) and components were visualized by ultraviolet light (254 nm). All the NMR spectra were recorded on Bruker Avance (Varian Unity Inova) spectrometer in $CDCl_3$ or DMSO-d_6 with TMS as internal standard. ^{1}H NMR and ^{13}C NMR spectra were recorded respectively at 400 MHz and 100 MHz, analyzed by using MestReNova Software. Chemical shifts were reported in ppm. Splitting patterns were expressed as s, singlet; d, doublet; t, triplet; q, quartet; dd, doublet of doublets; m, multiplet; brs, broad singlet. High resolution mass spectrometry (HRMS) was performed on an Agilent LC/MSD TOF system G3250AA. Silicycle silica gel 300−400 (particle size 40−63 μm) mesh was used for all flash column chromatography experiments.

4.1.1. *General procedures for the preparation of 2a-d*

To a solution of 2-acetylnaphtho[2,3-b]furan-4,9-dione **(1)** (0.42 mmol) in EtOH (5 mL), piperidine (1.25 mmol) and aromatic aldehydes (0.62 mmol) were added. The reaction mixture was heated to reflux and stirred for 7 hours, then cooled to room temperature. The mixture was filtered and the filter cake was washed with 10mL of

EtOH for three times, and dried under vacuum to give compounds **2a-d**.

*(E)-2-cinnamoylnaphtho[2,3-b]furan-4,9-dione(**2a**)*

^{1}H NMR (400 MHz, DMSO) δ 8.53 (s, 1H), 8.19 – 8.13 (m, 2H), 7.99 – 7.90 (m, 5H), 7.87 (d, *J* = 15.6 Hz, 1H), 7.52 – 7.48 (m, 3H).^{13}C NMR (100 MHz, Pyr) δ 179.8, 178.0, 174.0, 156.3, 153.5, 145.6, 134.6, 134.3, 134.2, 133.4, 133.0, 131.3, 130.9, 129.2 (2C), 129.2 (2C), 127.0, 126.9, 121.0, 113.7. HRMS (Q-TOF): calculated for $C_{21}H_{12}O_4$ 329.0736 $[M + H]^+$, found 329.0815. Purity ≥ 95.0%.

*(E)-2-(3-(1-methyl-1H-pyrrol-2-yl)acryloyl)naphtho[2,3-b]furan-4,9-dione(**2b**)*

^{1}H NMR (400 MHz, DMSO) δ 8.30 (s, 1H), 8.19 – 8.13 (m, 2H), 7.95 – 7.90 (m, 2H), 7.80 (d, *J* = 15.2 Hz, 1H), 7.52 (d, *J* = 15.2 Hz, 1H), 7.17 (d, *J* = 3.2 Hz, 2H), 6.25 – 6.23 (m, 1H), 3.80 (s, 3H).^{13}C NMR (100 MHz, DMSO) δ 180.4, 177.1, 174.1, 156.5, 153.7, 134.9 (2C), 133.4, 133.3, 133.0, 130.8, 130.6, 130.1, 127.1, 127.0, 115.4, 115.4, 114.0, 110.5, 34.5. HRMS (Q-TOF): calculated for $C_{21}H_{13}NO_4$ 332.0845 $[M + H]^+$, found 332.0905. Purity ≥ 95.0%.

*(E)-2-(3-(thiophen-2-yl)acryloyl)naphtho[2,3-b]furan-4,9-dione(**2c**)*

^{1}H NMR (400 MHz, DMSO) δ 8.44 (s, 1H), 8.20 – 8.13 (m, 2H), 8.05 (d, *J* = 15.4 Hz, 1H), 7.96 – 7.91 (m, 2H), 7.88 (d, *J* = 5.0 Hz, 1H), 7.79 (d, *J* = 3.4 Hz, 1H), 7.61 (d, *J* = 15.4 Hz, 1H), 7.24 (m, 1H).^{13}C NMR (100 MHz, DMSO) δ 180.2, 177.6, 174.1, 155.8, 153.9, 139.8, 138.1, 135.0, 134.9, 134.3, 133.4, 133.0, 132.2, 130.8, 129.4, 127.2, 127.0, 120.1, 115.0. HRMS (Q-TOF): calculated for $C_{19}H_{14}O_4S$ 335.0300 $[M + H]^+$, found 335.0385. Purity ≥ 95.0%.

*(E)-2-(3-([1,1'-biphenyl]-4-yl)acryloyl)naphtho[2,3-b]furan-4,9-dione(**2d**)*

^{1}H NMR (400 MHz, DMSO) δ 8.55 (s, 1H), 8.19 – 8.14 (m, 2H), 8.04 (m, 2H), 7.97 (d, *J* = 14.0 Hz, 1H), 7.94 (m, 2H), 7.90 (d, *J* = 10.2 Hz, 1H), 7.79 (m, 4H), 7.51 (t, *J* = 7.6 Hz, 2H), 7.42 (t, *J* = 7.4 Hz, 1H). ^{13}C NMR (100 MHz, DMSO) δ 180.3, 177.9, 174.2, 155.9, 154.1, 144.9, 143.2, 139.6, 135.0, 134.9, 133.8, 133.5, 133.1, 130.8, 130.4, 129.5, 128.6, 127.6, 127.3, 127.2, 127.1, 121.9, 115.5. HRMS (Q-TOF): calculated for $C_{27}H_{16}O_4$ 406.1082 $[M + H]^+$, found 406.2045. Purity ≥ 95.0%.

4.1.2. *Synthesis of 3-phenyliodonio-1, 2, 4-trioxo-1,2,3,4-tetrahydronaphthalenide (4)*

The synthesis of compound **4** was carried out according to the previously reported procedure [23].To a solution of 2-hydroxy-1,4-naphthoquinone **(3)** (5 g, 28.7mmol) in $CHCl_3$ (60 mL), iodobenzene diacetate (15 g, 46.6mmol) was added at room temperature. After the reaction mixture stirred at this temperature for 6 h, the mixture was filtered to give an orange precipitate, washed with $CHCl_3$ for three times and dried to afford compound **4** as orange solid (9.8 g, 91.0%).

4.1.3. ***Synthesis of 2-hydroxymethyl-naphtho[2,3-b]furan-4,9-dione (5)***

To a stirred solution of **4** (5.0 g, 13.3 mmol) in pyridine (60 mL), cuprous oxide (5.0 g) was added at room temperature. Then the reaction mixture was heated to 80 °C. The mixture solution was added propargyl alcohol (10 mL) slowly, and stirred at this temperature for 2.5 h. The solution was cooled to room temperature, filtered and diluted with 400 mL of 10% aqueous HCl. The acidic solution was extracted three times with 50 mL of EtOAc. The organic layer was washed with saturated copper sulfate solution and dried over anhydrous Na_2SO_4, filtered and concentrated under reduced pressure. The residue was purified by chromatography on Si gel column with DCM- MeOH to obtain compound **5** as an orange solid (540 mg, 17.8%).^{1}H NMR (400 MHz, DMSO) δ 8.14 – 8.04 (m, 2H), 7.94 – 7.81 (m, 2H), 6.94 (s, 1H), 5.72 (t, *J* = 4.8 Hz, 1H), 4.61 (d, *J* = 4.8 Hz, 2H).

4.1.4. ***Synthesis of 2-formyl-4,9-dihydronaphtho[2,3-b]-furan-4,9-dione (6)***

To a solution of **5** (500 mg, 2.19 mmol) in DCM (5 mL), pyridinium chlorochromate (1.5 g) was added. The mixture was stirred at room temperature for overnight. Then the solution was diluted with H_2O and extracted with DCM for three times. The combined organic phase was washed with brine and dried over anhydrous Na_2SO_4, filtered and concentrated under reduced pressure. The residue was purified by chromatography on Si gel column with DCM to give compound **6** as a yellow solid (398 mg, 80.4%).^{1}H NMR (400 MHz, DMSO) δ 9.91 (s, 1H), 8.23 – 8.09 (m, 2H), 8.04 (s, 1H), 7.98 – 7.86 (m, 2H).

4.1.5. ***Synthesis of 4,9-dioxo-4,9-dihydronaphtho[2,3-b]furan-2-carboxylic acid (7)***

The synthesis of intermediate compound 7 was carried out according to the previously reported procedure [19].To a solution of 6 (300 mg, 1.33 mmol) in glacial

HOAc (20 mL), H_2O_2 (30%, 10 mL) was added at 75 °C, and the mixture was stirred at this temperature for 4 h. Then it was concentrated under reduced pressure, and the residue was filtered and washed with H_2O for three times, and dried in a vacuum dryer to afford compound 7 as a yellow solid (289 mg, 90.0%).^{1}H NMR (400 MHz, DMSO) δ 14.17 (brs, 1H), 8.40 – 8.05 (m, 2H), 8.02 – 7.84 (m, 2H), 7.68 (s, 1H).

4.1.6. ***General procedures for the preparation of 8a-u***

The solution of intermediate compound 7 (0.20 mmol) in DCM (3 mL) was stirred with HATU (0.31 mmol) at room temperature for 10 minutes and then triethylamine (0.31 mmol), substituted alkyl amines or N-heterocycles (0.36 mmol) was added. After the reaction mixture stirred at room temperature for 2h, the mixture was evaporated under vacuum, purified by chromatography on Si gel column with DCM to afford compounds **8a-u**.

*2-(pyrrolidine-1-carbonyl)naphtho[2,3-b]furan-4,9-dione(**8a**)*

^{1}H NMR (400 MHz, $CDCl_3$) δ 8.16 – 8.10 (m, 2H), 7.95 – 7.88 (m, 2H), 7.55 (s, 1H), 3.81 (t, *J* = 6.8 Hz, 2H), 3.52 (t, *J* = 6.8 Hz, 2H), 1.95 (m, 2H), 1.91 – 1.83 (m, 2H).^{13}C NMR (100 MHz, DMSO) δ 180.4, 173.8, 156.4, 152.6, 152.5, 134.9, 134.9, 133.3, 132.8, 130.4, 127.1, 127.0, 111.7, 48.2, 47.5, 26.4, 23.8. HRMS (Q-TOF): calculated for $C_{17}H_{13}NO_4$ 318.0845 $[M + Na]^+$, found 318.0705. Purity ≥ 95.0%.

*2-(piperidine-1-carbonyl)naphtho[2,3-b]furan-4,9-dione (**8b**)*

^{1}H NMR (400 MHz, DMSO) δ 8.17 – 8.09 (m, 2H), 7.95 – 7.88 (m, 2H), 7.44 (s, 1H), 3.71 – 3.54 (m, 4H), 1.61 (m, 6H).^{13}C NMR (100 MHz, DMSO) δ 180.4, 173.7, 157.7, 152.3, 152.2, 134.9, 134.8, 133.3, 132.8, 130.2, 127.1, 126.9, 110.7, 47.9, 43.5, 26.7, 25.7, 24.3. HRMS (Q-TOF): calculated for $C_{18}H_{15}NO_4$ 310.1001 $[M + H]^+$, found 310.1030. Purity ≥ 95.0%.

*2-(morpholine-4-carbonyl)naphtho[2,3-b]furan-4,9-dione (**8c**)*

^{1}H NMR (400 MHz, DMSO) δ 8.17 – 8.08 (m, 2H), 7.92 – 7.87 (m, 2H), 7.53 (s, 1H), 3.68 (s, 8H). ^{13}C NMR (100 MHz, DMSO) δ 180.3, 173.7, 157.9, 152.5, 151.4, 134.9, 134.9, 133.3, 132.7, 130.2, 127.1, 126.9, 111.6, 66.6, 66.5, 66.5, 66.5. HRMS (Q-TOF): calculated for $C_{17}H_{13}NO_5$ 334.0794 $[M + Na]^+$, found 334.0603. HPLC purity 100.0%.

*2-(thiomorpholine-4-carbonyl)naphtho[2,3-b]furan-4,9-dione (**8d**)*

^{1}H NMR (400 MHz, DMSO) δ 8.19 – 8.05 (m, 2H), 8.01 – 7.85 (m, 2H), 7.48 (s, 1H), 3.90 (m, 4H), 2.82 – 2.68 (m, 4H).^{13}C NMR (100 MHz, DMSO) δ 180.3, 173.7, 158.2, 152.4, 151.6, 134.9, 134.9, 133.3, 132.7, 130.2, 127.1, 126.9, 111.2, 27.7, 27.5, 27.3, 27.2. HRMS (Q-TOF): calculated for $C_{17}H_{13}NO_4S$ 350.0564 $[M + Na]^+$, found 350.0402. HPLC purity ≥ 99.3%.

*2-(4-methylpiperazine-1-carbonyl)naphtho[2,3-b]furan-4,9-dione (**8e**)*

^{1}H NMR (400 MHz, DMSO) δ 8.15 – 8.09 (m, 2H), 7.94 – 7.87 (m, 2H), 7.48 (s, 1H), 3.67 (s, 4H), 2.41 – 2.37 (m, 4H), 2.22 (s, 3H).^{13}C NMR (100 MHz, DMSO) δ 180.3, 173.7, 157.7, 152.4, 151.7, 134.9, 134.8, 133.2, 132.7, 130.2, 127.1, 126.9, 111.3, 55.3, 54.6, 46.8, 46.0, 42.6. HRMS (Q-TOF): calculated for $C_{18}H_{16}N_2O_4$ 347.1110 $[M+ Na]^+$, found 347.0997. HPLC purity ≥ 99.5%

*2-(4-ethylpiperazine-1-carbonyl)naphtho[2,3-b]furan-4,9-dione (**8f**)*

^{1}H NMR (400 MHz, DMSO) δ 8.16 – 8.09 (m, 2H), 7.96 – 7.87 (m, 2H), 7.49 (s, 1H), 3.67 (s, 4H), 2.46 – 2.42 (m, 4H), 2.38 (q, *J* = 7.2 Hz, 2H), 1.02 (t, *J* = 7.2 Hz, 3H).^{13}C NMR (100 MHz, DMSO) δ 180.3, 173.7, 157.7, 152.4, 151.7, 134.9, 134.8, 133.2, 132.7, 130.2, 127.1, 126.9, 111.3, 53.1, 52.3, 51.8, 47.0, 42.7, 12.3. HRMS (Q-TOF): calculated for $C_{19}H_{18}N_2O_4$ 339.1267 $[M + H]^+$, found: 339.1235. HPLC purity ≥ 99.8%

*2-(4-oxopiperidine-1-carbonyl)naphtho[2,3-b]furan-4,9-dione (**8g**)*

^{1}H NMR (400 MHz, DMSO) δ 8.17 – 8.10 (m, 2H), 7.94 – 7.87 (m, 2H), 7.57 (s, 1H), 3.96 (brs, 4H), 2.55 (t, *J* = 6.4 Hz,4H).^{13}C NMR (100 MHz, DMSO) δ 207.3, 180.4, 173.7, 158.3, 152.5, 151.6, 134.9, 134.9, 133.3, 132.8, 130.2, 127.1, 126.9, 111.6, 44.6, 41.4, 40.8, 39.5. HRMS (Q-TOF): calculated for $C_{18}H_{13}NO_5$ 324.0794 $[M + H]^+$, found 324.0898. HPLC purity ≥ 99.4%

*Methyl-2-(1-(4,9-dioxo-4,9-dihydronaphtho[2,3-b]furan-2-carbonyl)piperidin-4-yl)acetate (**8h**)*

^{1}H NMR (400 MHz, DMSO) δ 8.16 – 8.10 (m, 2H), 7.91 (m, 2H), 7.44 (s, 1H), 4.39 (m, 1H), 4.09 – 4.00 (m, 1H), 3.60 (s, 3H), 3.25 (m, 1H), 2.94 – 2.83 (m, 1H), 2.32 (d, *J* = 7.0 Hz, 2H), 2.08 – 1.98 (m, 1H), 1.82 – 1.72 (m, 2H), 1.31 – 1.15 (m,

2H).^{13}C NMR (100 MHz, DMSO) δ 180.4, 173.7, 172.7, 157.7, 152.3, 152.1, 134.9, 134.8, 133.3, 132.8, 130.2, 127.1, 126.9, 110.9, 51.7, 46.9, 42.6, 40.2, 32.8, 32.3, 31.4. HRMS (Q-TOF): calculated for $C_{21}H_{19}NO_6$ 382.1212 $[M + H]^+$, found: 382.1282. Purity ≥ 95.0%.

*2-(4-(3-chlorophenyl)piperidine-1-carbonyl)naphtho[2,3-b]furan-4,9-dione (**8i**)*

^{1}H NMR (400 MHz, $CDCl_3$) δ 8.28 – 8.19 (m, 2H), 7.84 – 7.76 (m, 2H), 7.45 (s, 1H), 7.26 (s, 1H), 7.23 – 7.20 (m, 2H), 7.13 – 7.10 (m, 1H), 4.83 (brs, 1H), 4.44 (brs, 1H), 3.35 (brs, 1H), 2.93 (brs, 1H), 2.85 (m, 1H), 2.01 (m, 2H), 1.78 (m, 2H).^{13}C NMR (100 MHz, DMSO) δ 180.4, 173.7, 157.8, 152.4, 152.0, 148.4, 134.9, 134.8, 133.6, 133.3, 132.8, 130.8, 130.3, 127.3, 127.1, 126.9, 126.8, 126.1, 110.9, 47.2, 44.4, 43.1, 41.8 , 32.8. HRMS (Q-TOF): calculated for $C_{24}H_{18}ClNO_4$ 442.0924 $[M + Na]^+$, found 442.0811. Purity ≥ 95.0%.

*2-(4-(4-fluorophenyl)piperidine-1-carbonyl)naphtho[2,3-b]furan-4,9-dione (**8j**)*

^{1}H NMR (400 MHz, DMSO) δ 8.17 – 8.10 (m, 2H), 7.95 – 7.88 (m, 2H), 7.51 (s, 1H), 7.36 – 7.31 (m, 2H), 7.16 – 7.09 (m, 2H), 4.58 (brs, 1H), 4.20 (brs, 1H), 3.49 (brs, 1H), 2.92 (m, 2H), 1.85 (brs, 2H), 1.69 (brs, 2H).^{13}C NMR (100 MHz, DMSO) δ 180.4, 173.7, 162.5, 160.1, 157.8, 152.4, 152.0, 142.0, 134.9, 133.3, 132.8, 130.2, 129.1, 129.0, 127.1, 126.9, 115.6, 115.4, 110.9, 47.6, 43.2, 41.3, 33.7, 33.2. HRMS (Q-TOF): calculated for $C_{24}H_{18}FNO_4$ 426.1220 $[M + Na]^+$, found: 426.1106. Purity ≥ 95.0%.

*2-(4-(4-methoxyphenyl)piperidine-1-carbonyl)naphtho[2,3-b]furan-4,9-dione(**8k**)*

^{1}H NMR (400 MHz, DMSO) δ 8.15 – 8.10 (m, 2H), 7.93 – 7.87 (m, 2H), 7.50 (s, 1H), 7.20 (d, *J* = 8.6 Hz, 2H), 6.87 (d, *J* = 8.6 Hz, 2H), 4.57 (brs, 1H), 4.19 (brs, 1H), 3.72 (s, 3H), 3.36 (brs, 1H), 2.94 (brs, 1H), 2.88 – 2.78 (m, 1H), 1.84 (m, 2H), 1.66 (m, 2H).^{13}C NMR (100 MHz, DMSO) δ 180.4, 173.7, 158.2, 157.8, 152.3, 152.1, 137.8, 134.9, 134.8, 133.3, 132.8, 130.2, 128.1 (2C), 127.1, 126.9, 114.3 (2C), 110.9, 55.5, 47.6, 43.3, 41.2, 33.6, 33.4. HRMS (Q-TOF): calculated for $C_{25}H_{21}NO_5$ 438.1420 $[M + Na]^+$, found: 438.1308. Purity ≥ 95.0%.

*2-(4-(3-(trifluoromethyl)phenyl)piperazine-1-carbonyl)naphtho[2,3-b]furan-4,9-dione (**8l**)*

^{1}H NMR (400 MHz, DMSO) δ 8.17 – 8.10 (m, 2H), 7.94 – 7.88 (m, 2H), 7.56 (s, 1H), 7.46 (t, *J* = 7.6 Hz, 1H), 7.27 (d, *J* = 7.6 Hz, 1H), 7.23 (s, 1H), 7.11 (d, *J* = 7.6 Hz, 1H), 3.86 (s, 4H), 3.41 – 3.36 (m, 4H). ^{13}C NMR (100 MHz, DMSO) δ 180.4, 173.7, 157.8, 152.5, 151.5, 151.2, 134.9, 134.9, 133.3, 132.8, 130.6, 130.3, 130.2, 127.1, 126.9, 119.6, 115.5, 111.8, 111.7, 48.2, 46.6, 42.4, 40.6. HRMS (Q-TOF): calculated for $C_{24}H_{17}F_3N_2O_4$ 455.1140 $[M + H]^+$, found: 455.1151. Purity ≥ 95.0%.

*N-(4,4-dimethylcyclohexyl)-4,9-dioxo-4,9-dihydronaphtho[2,3-b]furan-2-carboxamid e (**8m**)*

^{1}H NMR (400 MHz, DMSO) δ 8.72 (d, *J* = 8.0 Hz, 1H), 8.17 – 8.09 (m, 2H), 7.94 – 7.88 (m, 2H), 7.67 (s, 1H), 3.74 (m, 1H), 1.67 – 1.52 (m, 4H), 1.41 (m, 2H), 1.32 – 1.21 (m, 2H), 0.93 (d, *J* = 9.4 Hz, 6H).^{13}C NMR (100 MHz, DMSO) δ 180.4, 173.8, 156.1, 152.7, 152.6, 134.9, 134.8, 133.3, 132.9, 130.8, 127.0, 127.0, 110.2, 48.8, 38.0 (2C), 32.6, 29.8, 28.2 (2C), 24.6. HRMS (Q-TOF): calculated for $C_{21}H_{21}NO_4$ 374.1471 $[M + Na]^+$, found: 374.1358. Purity ≥ 95.0%.

*N-(adamantan-1-yl)-4,9-dioxo-4,9-dihydronaphtho[2,3-b]furan-2-carboxamide (**8n**)*

^{1}H NMR (400 MHz, DMSO) δ 8.19 – 8.07 (m, 2H), 8.02 (s, 1H), 7.91 (m, 2H), 7.75 (s, 1H), 2.08 (s, 9H), 1.67 (s, 6H).^{13}C NMR (100 MHz, DMSO) δ 180.5, 173.7, 156.3, 152.9, 152.5, 134.9, 134.8, 133.3 (s), 132.9, 130.7, 127.0, 127.0, 110.1, 52.8, 41.1 (3C), 36.4 (2C), 29.3 (4C). HRMS (Q-TOF): calculated for $C_{23}H_{21}NO_4$ 376.1471 $[M + H]^+$, found 376.1539. Purity ≥ 95.0%.

*N-cyclohexyl-4,9-dioxo-4,9-dihydronaphtho[2,3-b]furan-2-carboxamide (**8o**)*

^{1}H NMR (400 MHz, DMSO) δ 8.70 (d, *J* = 8.0 Hz, 1H), 8.17 – 8.08 (m, 2H), 7.94 – 7.88 (m, 2H), 7.68 (s, 1H), 3.77 (m, 1H), 1.82 (m, 1H), 1.77 – 1.71 (m, 2H), 1.61 (m, 2H), 1.37 – 1.31 (m, 3H), 1.23 (m, 2H).^{13}C NMR (100 MHz, DMSO) δ 180.4, 173.8, 156.1, 152.7, 152.6, 134.9, 134.8, 133.3, 132.9, 130.7, 127.0, 127.0, 110.2, 48.9, 32.6 (2C), 25.3 (2C). HRMS (Q-TOF): calculated for $C_{19}H_{17}NO_4$ 324.1158 $[M + H]^+$, found: 324.1235. Purity ≥ 95.0%.

*4,9-dioxo-N-(2-(pyrrolidin-1-yl)ethyl)-4,9-dihydronaphtho[2,3-b]furan-2-carboxamid e(**8p**)*

^{1}H NMR (400 MHz, DMSO) δ 8.88 (t, *J* = 5.8 Hz, 1H), 8.18 – 8.08 (m, 2H),

7.96 – 7.86 (m, 2H), 7.63 (s, 1H), 3.40 (q, *J* = 6.6 Hz, 2H), 2.59 (t, *J* = 6.6 Hz, 2H), 2.49 (m, 4H), 1.76 – 1.60 (m, 4H).^{13}C NMR (100 MHz, DMSO) δ 180.4, 173.8, 156.9, 152.7, 152.5, 134.9, 134.8, 133.3, 132.9, 130.7, 127.1, 127.0, 110.3, 55.1 (2C), 54.1, 38.8 (2C), 23.6. HRMS (Q-TOF): calculated for $C_{19}H_{18}N_2O_4$ 339.1267 $[M + H]^+$, found 339.1348. Purity ≥ 95.0%.

4,9-dioxo-N-(2-(piperidin-1-yl)ethyl)-4,9-dihydronaphtho[2,3-b]furan-2-carboxamide ***(8q)***

^{1}H NMR (400 MHz, DMSO) δ 8.83 (t, *J* = 5.8 Hz, 1H), 8.18 – 8.08 (m, 2H), 7.94 – 7.86 (m, 2H), 7.62 (s, 1H), 3.39 (q, *J* = 6.6 Hz, 2H), 2.44 (t, *J* = 6.6 Hz, 2H), 2.38 (m, 4H), 1.49 (m, 4H), 1.41 – 1.34 (m, 2H).^{13}C NMR (100 MHz, DMSO) δ 180.4, 173.8, 156.9, 152.7, 152.5, 134.9, 134.8, 133.3, 132.9, 130.7, 127.1, 127.0, 110.2, 57.9, 54.5 (2C), 37.1, 26.0 (2C), 24.5. HRMS (Q-TOF): calculated for $C_{20}H_{20}N_2O_4$ 353.1423 $[M + H]^+$, found 353.1504. HPLC purity ≥ 98.8%

N-(2-morpholinoethyl)-4,9-dioxo-4,9-dihydronaphtho[2,3-b]furan-2-carboxamide ***(8r)***

^{1}H NMR (400 MHz, DMSO) δ 8.87 (t, *J* = 5.6 Hz, 1H), 8.19 – 8.09 (m, 2H), 7.96 – 7.87 (m, 2H), 7.63 (s, 1H), 3.61 – 3.54 (m, 4H), 3.41 (q, *J* = 6.6 Hz, 2H), 2.47 (t, *J* = 6.6 Hz, 2H), 2.42 (m, 4H).^{13}C NMR (100 MHz, DMSO) δ 180.4, 173.8, 156.9, 152.7, 152.5, 134.9, 134.8, 133.3, 132.9, 130.7, 127.1, 127.0, 110.3, 66.7 (2C), 57.6, 53.7 (2C), 36.7. HRMS (Q-TOF): calculated for $C_{19}H_{18}N_2O_5$ 355.1216 $[M + H]^+$, found: 355.1290. HPLC purity ≥ 98.8%

*4,9-dioxo-N-phenethyl-4,9-dihydronaphtho[2,3-b]furan-2-carboxamide (****8s****)*

^{1}H NMR (400 MHz, DMSO) δ 9.03 (t, *J* = 5.6 Hz, 1H), 8.16 – 8.08 (m, 2H), 7.95 – 7.86 (m, 2H), 7.60 (s, 1H), 7.26 (m, 5H), 3.57 – 3.48 (q, *J* = 7.4 Hz, 2H), 2.87 (t, *J* = 7.4 Hz, 2H).^{13}C NMR (100 MHz, DMSO) δ 180.3, 173.8, 156.9, 152.7, 152.5, 139.6, 134.9, 134.8, 133.3, 132.8, 130.7, 129.1 (2C), 128.9 (2C), 127.0, 127.0, 126.7, 110.2, 41.0, 35.3. HRMS (Q-TOF): calculated for $C_{21}H_{15}NO_4$ 368.1001 $[M + Na]^+$, found: 368.0698. Purity ≥ 95.0%.

*N-(4-chlorophenethyl)-4,9-dioxo-4,9-dihydronaphtho[2,3-b]furan-2-carboxamide (****8t****)*

^{1}H NMR (400 MHz, DMSO) δ 9.01 (t, *J* = 5.6 Hz, 1H), 8.17 – 8.08 (m, 2H),

7.94 – 7.87 (m, 2H), 7.61 (s, 1H), 7.38 – 7.33 (m, 2H), 7.30 – 7.26 (m, 2H), 3.52 (q, 7.2 Hz, 2H), 2.86 (t, *J* = 7.2 Hz, 2H).^{13}C NMR (100 MHz, DMSO) δ 180.4, 173.8, 156.9, 152.7, 152.4, 138.7, 134.9, 134.8, 133.3, 132.9, 131.3, 131.1 (2C), 130.7, 128.7 (2C), 127.1, 127.0, 110.3, 40.7, 34.5. HRMS (Q-TOF): calculated for $C_{21}H_{14}ClNO_4$ 380.0611 $[M + H]^+$, found: 380.0690. Purity ≥ 95.0%.

*N-(4-methoxyphenethyl)-4,9-dioxo-4,9-dihydronaphtho[2,3-b]furan-2-carboxamide(**8u**)*

^{1}H NMR (400 MHz, DMSO) δ 8.99 (t, *J* = 5.6 Hz, 1H), 8.17 – 8.07 (m, 2H), 7.96 – 7.86 (m, 2H), 7.61 (s, 1H), 7.16 (d, *J* = 8.4 Hz, 2H), 6.86 (d, *J* = 8.4 Hz, 2H), 3.72 (s, 3H), 3.48 (q, *J* = 7.4 Hz, 2H), 2.80 (t, *J* = 7.4 Hz, 2H).^{13}C NMR (100 MHz, DMSO) δ 180.4, 173.8, 158.2, 156.9, 152.7, 152.5, 134.9, 134.8, 133.3, 132.9, 131.5, 130.7, 130.1 (2C), 127.0, 127.0, 114.3 (2C), 110.2, 55.5, 41.2, 34.5. HRMS (Q-TOF): calculated for $C_{22}H_{17}NO_5$ 398.1107 $[M + Na]^+$, found: 398.1009. Purity ≥ 95.0%.

4.2. *In vitro* inhibitory activity

U251, HepG2, HT29, CT26 and PC-3 cells were seeded in 96-well plates at a density of 5×10^3 cells/well and cultured for 24 h. Following the addition of different concentrations of compounds, the cells were further cultured for 72 h, with 0.5% DMSO as the solvent control group. Then cells were incubated for 4 h with 5mg/ml of 3-(4,5-dimethylthiazol-2-yl)-2,5-diphenyltetrazolium bromide (MTT) solution, and the formazan crystals were dissolved with 150ul of DMSO. After gentle shaking for 10min, the optical density (OD) was measured at 570nm using a Spectra MAX M5 microplate spectrophotometer. Each treatment was performed in triplicate. Results were analyzed with GraphPad Prism 6 and data were shown as Mean ± SD.

4.3. Molecular docking

Molecular docking studies were carried out using the Discovery Studio (DS) 3.1 software. The protein was constructed based on the X-ray structure of STAT3, which was available through the RCSB Protein Data Bank (PDB code: 1BG1). Both the compounds and the structure of STAT3 were prepared and optimized using Discovery Studio 3.1. The protein was prepared with adding hydrogens, deleting water molecules. The low energy clusters were identified and binding energies were

evaluated.

4.4. The determination of aqueous solubility

The aqueous solubility of the compounds **8c-g, 8q** and **8r** were determined by HPLC method. The calibration standards were prepared with concentrations for 15, 25, 50, 75, 100, 125 μg/mL and used to assess calibration curves. The compounds (2 mg) were added into 1.5 mL EP tubes respectively. The pure water (1 mL) was added into each EP tube. Then the EP tubes were vortexed for 30s and swung at room temperature for 24 h to obtain saturated solution, which were disposed by HPLC system.

4.5. *In Vivo* Antitumor Activity Evaluation

CT-26 cells (1×10^6) were subcutaneously implanted in the right flanks of 6-week-old male BALB/c mice, which were purchased from DaShuo experimental animal Co. Ltd. (Chengdu, Sichuan, China). After the solid tumors volume were reached about 70 mm^3, mice were randomized to two groups with five mice per group and were orally administrated with **8q** 50mg/kg and vehicle per day. Compound **8q** was dissolved at 5% 1-methyl-2-pyrrolidinone in polyethylene glycol 400, and the blank control group received oral administration of equal volume of 5% NMP, 95% PEG. The tumors were measured every 3 days with a caliper. Tumor volume (V) was estimated using the equation $V = ab^2/2$, where a and b stand for the longest and shortest diameter, respectively. After treatment, mice were sacrificed and dissected to weigh the tumor tissues and to examine the internal organ injury by macroscopic analysis. TGI and T/C were calculated according to the following formula:

TGI = (the mean tumor weight of control group - the mean tumor weight of treated group)/ (the mean tumor weight of control group).

T /C=mean RTV of treated group/mean RTV of control group

RTV, namely, relative tumor volume, is V_t/ V_0 (Vt is the tumor volume measured at the end of treatment; V_0 is the tumor volume measured at the beginning of treatment).

4.6. Western blot and immunofluorescence analysis

Total cellular proteins were extracted in RIPA buffer (Beyotime Biotechnology) supplemented with protease inhibitor cocktail (Sigma-Aldrich). Protein concentrations

were determined with BCA protein assay kit (Thermo Fisher Scientific). Equal amounts of protein were run out on 10% SDS-PAGE gel and subsequently transferred onto PVDF membranes (Millipore). Membranes were blocked in 5% skimmed milk and incubated with the following primary antibodies at 4□ overnight: mouse monoclonal antibody to total STAT3 (Cell Signaling, 1:1000, #9139), rabbit monoclonal antibody to p-STAT3 (Tyr705) (Cell Signaling, 1:1,000, #9145) and rabbit polyclonal antibody to GADPH (BOSTER, 1:500, BA2913). Second antibodies were from Beyotime Biotech and used at a dilution of 1:2,000. Enhanced chemiluminescence (ECL) and digital imaging (Clinx Science Instruments, Chemiscope 5300) were used for detection of target proteins. For immunofluorescence analysis, the primary antibody of total STAT3 was the same as used in western blot. Cell nucleus was stained with DAPI (Roche). Images were taken on a Zeiss microscope (Axio Observer).

4.7. Total STAT3 and p-STAT3^{Y705} sandwich enzyme-linked immunosorbent assay

Whole-cell lysates were prepared using cell lysis buffer (Beyotime Biotechnology) containing protease inhibitor cocktail (Sigma-Aldrich). Protein concentrations were quantified with BCA protein assay kit (Thermo Fisher Scientific). Levels of total and p-STAT3^{Y705} were measuring by using PathScan Total Stat3 and Phospho-Stat3 (Tyr705) Sandwich ELISA Kit (Cell Signaling, 7305 & 7300) according to the manufacturer's instructions. The measurements were repeated three times. For statistical analyses, treatment groups were compared with control group by paired t-test and data are represented as means ± S.D.

4.8. Electrophoretic Mobility Shift Assay (EMSA)

HEK293T cells were transiently transfected with N-terminal FLAG-tagged STAT3 expression construct (10 μg/10 cm dish). Forty-eight hours post transfection, cells were harvested and dissolved in lysis buffer (500 μL/10 cm dish). After sonification and centrifugation, STAT3 were purified by Anti-FLAG M2 Magnetic Beads from Sigma (M8823) according to the instructions. Protein was eluted from beads with 200 μL flag peptide (200 μg/mL). EMSA was performed by using

Chemiluminescent EMSA Kit (GS009, Beyotime) according to the instructions. Biotin labeled STAT3 probe, cold probe and nylon membranes were also purchased from Beyotime (GS083B, FFN10). 5 μL eluted protein and 1 μL probe were loaded with each lane. Anti-total STAT3 antibody is the same as used in western blot. Enhanced chemiluminescence (ECL) and digital imaging (Clinx Science Instruments, Chemiscope 5300) were used for detection of target proteins. Compond **8q** was added as indicated.

4.9. Purification of STAT3 and Surface Plasmon Resonance (SPR) analysis

Full-length STAT3 with N-terminal His-tag was expressed by baculovirus in Sf9 insect cells. Briefly, STAT3 vector was co-transfected with Bac-N-Blue DNA into Sf9 cells. Recombinant virus was amplified in Sf9 cells and expressed in High Five cells. 2–3 d post-infection, cells were spun down and the medium was collected for purification. After filter, concentration and dialysis, protein was purified by Ni-NTA Agarose and gel-filtration columns. Protein purity (>90%) and concentration were determined by SDS-PAGE with Coomassie staining and UV spectrometry.

STAT3 and compound **8q** binding analyses was performed by using Biacore X100 (GE Healthcare, UK) according to standard methods. Protein was covalently immobilized to the surface of a CM5 sensor chip using a amine coupling kit (GE Healthcare). Compound **8q** was diluted with 5% DMSO in PBS buffer. The concentrations were set at 600, 300, 150, 75, 37.5 and 18.75 nM. The equilibrium dissociation constant (KD) was obtained by using the BIAevaluation 2.0 software.

Conflicts of interest

The authors declare no other conflicts of interest.

Acknowledgments

This work was supported by the National Natural Science Foundation of China (No.81473253), the National Mega-projects of China for Innovative Drugs (2018ZX09721001-001-001).

References

[1] J.E. Darnell Jr, STATs and Gene Regulation, *Science*, 277 (1997) 1630-1635.

[2] S. Haftchenary, M. Avadisian, P.T. Gunning, Inhibiting aberrant Stat3 function with molecular therapeutics: a progress report, *Anticancer Drugs*, 22 (2011) 115-127.

[3] S. Fletcher, J. Turkson, P.T. Gunning, Molecular approaches towards the inhibition of the signal transducer and activator of transcription 3 (Stat3) protein, *ChemMedChem*, 3 (2008) 1159-1168.

[4] H. Yu, H. Lee, A. Herrmann, R. Buettner, R. Jove, Revisiting STAT3 signalling in cancer: new and unexpected biological functions, *Nat Rev Cancer*, 14 (2014) 736-746.

[5] A. Xiong, Z. Yang, Y. Shen, J. Zhou, Q. Shen, Transcription Factor STAT3 as a Novel Molecular Target for Cancer Prevention, *Cancers (Basel)*, 6 (2014) 926-957.

[6] H. Chen, Z. Yang, C. Ding, L. Chu, Y. Zhang, K. Terry, H. Liu, Q. Shen, J. Zhou, Fragment-based drug design and identification of HJC0123, a novel orally bioavailable STAT3 inhibitor for cancer therapy, *Eur J Med Chem*, 62 (2013) 498-507.

[7] J. Schust, B. Sperl, A. Hollis, T.U. Mayer, T. Berg, Stattic: a small-molecule inhibitor of STAT3 activation and dimerization, *Chem Biol*, 13 (2006) 1235-1242.

[8] K. Matsuno, Y. Masuda, Y. Uehara, H. Sato, A. Muroya, O. Takahashi, T. Yokotagawa, T. Furuya, T. Okawara, M. Otsuka, N. Ogo, T. Ashizawa, C. Oshita, S. Tai, H. Ishii, Y. Akiyama, A. Asai, Identification of a New Series of STAT3 Inhibitors by Virtual Screening, *ACS Med Chem Lett*, 1 (2010) 371-375.

[9] H. Song, R. Wang, S. Wang, J. Lin, A low-molecular-weight compound discovered through virtual database screening inhibits Stat3 function in breast cancer cells, *Proc Natl Acad Sci U S A*, 102 (2005) 4700-4705.

[10] H. Chen, Z. Yang, C. Ding, L. Chu, Y. Zhang, K. Terry, H. Liu, Q. Shen, J. Zhou, Discovery of O-Alkylamino Tethered Niclosamide Derivatives as Potent and Orally Bioavailable Anticancer Agents, *ACS Med Chem Lett*, 4 (2013) 180-185.

[11] S.W. Yu Wang, Yansheng Wu, Yu Ren, Zhaoqing Li, Xiaofeng Yao, Chao Zhang, Na Ye,, J.D. Chao Jing, Kailiang Zhang, Shanshan Sun, Minghui Zhao, Wenyu Guo, Xin Qu, Yu Qiao,, L.K. Haiying Chen, Rui Jin, Xudong Wang, Lun Zhang, Jia Zhou, Qiang Shen, Xuan Zhou., Suppression of the Growth and Invasion of Human Head and Neck Squamous Cell Carcinomas

via Regulating STAT3 Signaling and miR-21/β-catenin Axis with HJC0152, *Mol Cancer Ther*, 16(4) (2017) 578-590.

[12] H. Chen, Z. Yang, C. Ding, A. Xiong, C. Wild, L. Wang, N. Ye, G. Cai, R.M. Flores, Y. Ding, Q. Shen, J. Zhou, Discovery of potent anticancer agent HJC0416, an orally bioavailable small molecule inhibitor of signal transducer and activator of transcription 3 (STAT3), *Eur J Med Chem*, 82 (2014) 195-203.

[13] L. Lin, B. Hutzen, P.-K. Li, S. Ball, M. Zuo, S. DeAngelis, E. Foust, M. Sobo, L. Friedman, D. Bhasin, L. Cen, C. Li, J. Lin, A Novel Small Molecule, LLL12, Inhibits STAT3 Phosphorylation and Activities and Exhibits Potent Growth-Suppressive Activity in Human Cancer Cells, *Neoplasia*, 12 (2010) 39-IN35.

[14] W. Yu, H. Xiao, J. Lin, C. Li, Discovery of novel STAT3 small molecule inhibitors via in silico site-directed fragment-based drug design, *J Med Chem*, 56 (2013) 4402-4412.

[15] S. Fiorito, F. Epifano, C. Bruyere, V. Mathieu, R. Kiss, S. Genovese, Growth inhibitory activity for cancer cell lines of lapachol and its natural and semi-synthetic derivatives, *Bioorg Med Chem Lett*, 24 (2014) 454-457.

[16] K.O. Eyong, P.S. Kumar, V. Kuete, G.N. Folefoc, E.A. Nkengfack, S. Baskaran, Semisynthesis and antitumoral activity of 2-acetylfuranonaphthoquinone and other naphthoquinone derivatives from lapachol, *Bioorg Med Chem Lett*, 18 (2008) 5387-5390.

[17] S. Bannwitz, D. Krane, S. Vortherms, T. Kalin, C. Lindenschmidt, N. Zahedi Golpayegani, J. Tentrop, H. Prinz, K. Muller, Synthesis and structure-activity relationships of lapacho analogues. 2. Modification of the basic naphtho[2,3-b]furan-4,9-dione, redox activation, and suppression of human keratinocyte hyperproliferation by 8-hydroxynaphtho[2,3-b]thiophene-4,9-diones, *J Med Chem*, 57 (2014) 6226-6239.

[18] J.M. Hubbard, A. Grothey, Napabucasin: An Update on the First-in-Class Cancer Stemness Inhibitor, *Drugs*, 77 (2017) 1091-1103.

[19] A. Reichstein, S. Vortherms, S. Bannwitz, J. Tentrop, H. Prinz, K. Muller, Synthesis and structure-activity relationships of lapacho analogues. 1. Suppression of human keratinocyte hyperproliferation by 2-substituted naphtho[2,3-b]furan-4,9-diones, activation by enzymatic one- and two-electron reduction, and intracellular generation of superoxide, *J Med Chem*, 55 (2012) 7273-7284.

[20] Q. Zhou, C. Peng, F. Du, L. Zhou, Y. Shi, Y. Du, D. Liu, W. Sun, M. Zhang, G. Chen, Design, synthesis and activity of BBI608 derivatives targeting on stem cells, *Eur J Med Chem,* 151 (2018) 39-50.

[21] A.W. Zhiwei Jiang, Hongwei Hu, Jiali Xu, Yuesong Hu., Novel esters of 4, 9-dihydroxy-naphtho [2, 3-B] furans for disease therapies, US20130345176A1, (2013).

[22] M. Kortylewski, M. Kujawski, T. Wang, S. Wei, S. Zhang, S. Pilon-Thomas, G. Niu, H. Kay, J. Mule, W.G. Kerr, R. Jove, D. Pardoll, H. Yu, Inhibiting Stat3 signaling in the hematopoietic system elicits multicomponent antitumor immunity, *Nature Med,* 11 (2005) 1314-1321.

[23] R.K.J. Chongming Wu, Michael R. Mattern, Jackson C. Wong, and David G. I. Kingston, Synthesis of Furanonaphthoquinones with Hydroxyamino Side Chains, *J Nat Prod,* 62 (1999).

Highlights

1. *In vitro*, compound **8q** was over 10-fold more potent than **napabucasin** on U251, HepG2, HT29 and CT26 cells.
2. In mouse model of colorectal cancer, **8q** significantly reduced tumor growth. The TGI of **8q** at 50 mg/kg was 63 %.
3. Compound **8q** has a K_D of 110.2 nM for full-length STAT3 recombinant protein by surface plasmon resonance analysis.
4. The aqueous solubility of **8q** was over 4.5-fold higher than that of **napabucasin**.
5. Compound **8q** exhibited good safety profile in BALB/c mice model.